Atmospheric Environment 144 (2016) 194–207

Contents lists available at ScienceDirect

Atmospheric Environment

journal homepage: www.elsevier.com/locate/atmosenv

Source apportionment of surface ozone in the Yangtze River Delta, China in the summer of 2013

L. Li [a, b, *], J.Y. An [a, b], Y.Y. Shi [a, c], M. Zhou [a, b], R.S. Yan [a, b], C. Huang [a, b], H.L. Wang [a, b], S.R. Lou [a, b], Q. Wang [a, b], Q. Lu [a, b], J. Wu [d]

[a] State Environmental Protection Key Laboratory of the Cause and Prevention of Urban Air Pollution Complex, Shanghai, 200233, China
[b] Shanghai Academy of Environmental Sciences, Shanghai, 200233, China
[c] School of Environmental Science and Engineering, Donghua University, Shanghai, 201620, China
[d] Environmental Science Research & Design Institute of Zhejiang Province, Hangzhou, 310007, China

HIGHLIGHTS

- A high O_3 episode over the YRD was simulated using the CAMx modeling system.
- Ozone source apportionment technology was applied to study the formation mechanism and sources of O_3.
- Contributions of different source regions and source categories to O_3 were analyzed.

ARTICLE INFO

Article history:
Received 7 May 2016
Received in revised form
23 August 2016
Accepted 29 August 2016
Available online 30 August 2016

Keywords:
Ozone
Source apportionment
Yangtze River Delta

ABSTRACT

We applied ozone source apportionment technology (OSAT) with tagged tracers coupled within the Comprehensive Air Quality Model with Extensions (CAMx) to study the region and source category contribution to surface ozone in the Yangtze River Delta area in summer of 2013. Results indicate that the daytime ozone concentrations in the YRD region are influenced by emissions both locally, regionally and super-regionally. At urban Shanghai, Hangzhou and Suzhou receptors, the ozone formation is mainly VOC-limited, precursor emissions form Zhejiang province dominate their O_3 concentrations. At the junction area among two provinces and Shanghai city, the ozone is usually influenced by all the three areas. The daily max O_3 at the Dianshan Lake in July are contributed by Zhejiang (48.5%), Jiangsu (11.7%), Anhui (11.6%) and Shanghai (7.4%), long-range transport constitutes around 20.9%. At Chongming site, the BVOC emissions rate is higher than urban region. Regional contribution results show that Shanghai constitutes 15.6%, Jiangsu contributes 16.2% and Zhejiang accounts for 25.5% of the daily max O_3. The analysis of the source category contribution to high ozone in the Yangtze River Delta region indicates that the most significant anthropogenic emission source sectors contributing to O_3 pollution include industry, vehicle exhaust, although the effects vary with source sector and selected pollution episodes. Emissions of NO_x and VOCs emitted from the fuel combustion of industrial boilers and kilns, together with VOCs emissions from industrial process contribute a lot to the high concentrations in urban Hangzhou, Suzhou and Shanghai. The contribution from regional elevated power plants cannot be neglected, especially to Dianshan Lake. Fugitive emissions of volatile pollution sources also have certain contribution to regional O_3. These results indicate that the regional collaboration is of most importance to reduce ambient ozone pollution, particularly during high ozone episodes.

1. Introduction

With the fast development of urbanization, industrialization and mobilization, the air pollutant emissions with photochemical reactivity become more obvious, causing a severe photochemical pollution situation in summer in the Yangtze River Delta (YRD)

* Corresponding author. Shanghai Academy of Environmental Sciences, Shanghai, 200233. China.
E-mail address: lili@saes.sh.cn (L. Li).

http://dx.doi.org/10.1016/j.atmosenv.2016.08.076
1352-2310/

region (Geng et al., 2007; Shi et al., 2015). Ozone (O_3) is a secondary pollutant which is mainly formed through the photochemical reactions between nitrogen oxides (NO_x) and volatile organic compounds (VOCs) under influence of sunlight (Chen et al., 2013; Huang et al., 2013; Liu et al., 2013; Zhang et al., 2011). High tropospheric ozone concentrations have a strong impact on human health (Liu et al., 2013; Shao et al., 2006; Streets et al., 2007) and significantly damage the environment (Feng et al., 2014). Therefore, the ozone pollution has attracted much attention around the world (Ding et al., 2013; Marais et al., 2014; Xie et al., 2014). Due to the high nonlinear relationship between O_3 and its precursor gases (Xing et al., 2011), figuring out the sources of high ozone is quite complicated. Many researchers have done quite a lot of studies on the sources of O_3. For example, Kim et al. (2009) applied High-Order Decoupled Direct Method (HDDM) in the Community Multi-scale Air Quality Modeling System (CMAQ) (Byun and Schere, 2006; Foley et al., 2010) to analyze the sources of ozone precursors and their impact on ozone formation in Dallas Fort Worth area. Li et al. (2011) studied the roles of NOx and VOCs precursors with the application of indicators like H_2O_2/HNO_3 and O_3/NOz in Shanghai. Li et al. (2012) applied process analysis to examine the formation and transport of high ozone in YRD. Wang et al. (2009) also applied ozone source apportionment technology (OSAT) and regional ozone assessment techniques (GOAT) available in Comprehensive Air Quality Model with Extensions (CAMx, ENVIRON, 2015) to quantify the ozone contributions in Beijing and its surrounding area. Li et al. (2012) analyzed the sources of near-ground ozone in the Pearl River Delta region by using OSAT, and results showed that regional transport made a significant contribution to high ozone events. These studies provide a critical insight into the prevention and control of ozone pollution.

However, studies on the formation process and source apportionment of summertime high O_3 in the YRD are still quite limited. Yangtze River Delta is one of the most important city-clusters in China, including Shanghai city, Jiangsu, Zhejiang and Anhui provinces. It occupies only 3.5% of the national total land territory (Wikipedia, 2014), but accounts for 16.1% of the total population (NBSC, 2013), and produces 24.3% of the domestic product (GDP) (NBSC, 2013). It takes an account of 17.7% of the total energy consumption (NBSC, 2013), 19.1% of the vehicle stock (NBSC, 2013), 22.3% of the power generation (NBSC, 2013), 20.4% of steel production and 18.2% of cement production in China (NBSC, 2013). Meanwhile, the air pollutant emissions in this region are quite large (Fu et al., 2013; Huang et al., 2011; Li et al., 2011a,b) compared with other regions. Based on the INTEX-B inventory (Zhang et al., 2009) for the year 2006, the YRD region contributes 14.3% of total SO_2, 18.9% of NO_x, 15.8% of $PM_{2.5}$ and 19.8% of total VOCs emissions in China. In comparison, the Beijing-Tianjin-Hebei region (JJJ) only constitutes 9.2%, 9.6, 8.9 and 10.3% of the SO_2, NO_x, $PM_{2.5}$ and VOCs national emissions, respectively (Zhang et al., 2009). Under influence of unfavorable meteorological conditions, the regional air quality is usually very bad, showing low visibility and haze in winter and high O_3 in summer. During July–August 2013, the YRD region experienced a high ozone pollution episode. Ground observational data show that the maximum hourly concentration reaching 276 ppb, 175 ppb and 135 ppb in the three cities, which are 1.9–3 times of the national ambient air quality standard (NAAQs) Grade II (hourly average limit: 200 $\mu g\ m^{-3}$, around 93 ppb). This pollution event shows an obvious regional photochemical pollution situation.

In this study, we focused on this high ozone pollution episode occurred in YRD during the summer season in 2013, and investigated the major source categories and source regions of O_3 formation to shed light on possible reasons. CAMx photochemical grid model with the Carbon Bond chemical mechanism (Gery et al., 1989) version 5 (CB05) is used to reproduce the pollution event, and the OSAT coupled within CAMx is applied to analyze the O_3 source apportionment at typical sites in YRD. This is undertaken to identify the dominant source types and source regions contributing to ozone. The YRD domain for CAMx has 156 × 186 horizontal grid cells and includes three provinces and Shanghai, which are also shown in Fig. 1. In this paper, the ozone contributions from 5 different regions (Shanghai, Zhejiang, Jiangsu, Anhui and long-range transport and 8 precursor emission source categories (power plants, industrial process, industrial boilers and kilns, mobile source, volatile source, residential, agricultural and biogenic emissions) to O_3 at 7 representative sites of the YRD are discussed. Results are helpful to provide scientific and technological support for the prevention and control of ozone in the eastern coastal city clusters.

2. Methodology

2.1. Model description

In this study, we applied Weather Research and Forecasting Model (WRF Version 3.7, Michalakes et al., 2001)-CAMx (Version6.1, ENVIRON, 2015) modeling system to reproduce the high ozone pollution episode in the YRD region in July, 2013. Fig. 1 shows the nested modeling domain with grid resolutions of 36 km × 36 km, covering the whole East and Southeast Asia; 12 km × 12 km, covering eastern China; 4 km × 4 km, covering Shanghai, Zhejiang, Jiangsu and Anhui provinces.

To differentiate the contributions from various precursor emission regions and source categories to ozone in the YRD region, we applied OSAT to do this study. OSAT (Yarwood et al., 1996) is an integrated approach of sensitivity analysis, which provides a reactive tracer method for estimating the contributions of multiple source areas, categories, and pollutant types to ozone formation. OSAT provides information about the relationships between ozone concentrations and sources of precursors in the formation of ozone. Ozone formation from VOCs and NOx precursors is tracked separately. It determines whether ozone formation is NOx or VOCs limited in each grid cell at each time step, and attributes ozone production according to the relative contributions of the limiting precursor (VOCs or NOx) from different sources present at that time. Likewise, the ozone contributions are tracked using a reactive tracer approach and separate tracers are used to track ozone formation attributed to NOx (O_3N tracers) and VOCs (O_3V tracers). Detailed description on the tracers, formulations, the advantages and limitations related to OSAT have been described in detail in other publications (Li et al., 2013; Zhang et al., 2005).

2.2. Model inputs

The inputs for the WRF were taken from 1° × 1° global reanalysis data of the National Centers for Environmental Prediction (NCEP). The gas-phase chemical reaction mechanism used in the CAMx model is CB05 (Foley et al., 2010; Yarwood et al., 2005). The vertical tropospheric levels used in CAMx is 15 layers from surface up to 100 hpa. The simulation period is from June 25, 2013 to July 31, 2013. We analyze the predicted results during July 01-July 31, 2013. Initial conditions (ICs) are prepared by running the model five days ahead of the start date. The boundary conditions (BCs) for the nested domains are extracted from the CAMx concentration files of the larger domain.

The source regions are divided into 5 areas, including Shanghai, Jiangsu, Zhejiang, Anhui and long-range transport. The contributions from ICs, boundary conditions (including NorthBC, SouthBC, WestBC, EastBC, TopBC) are defined as long-range transport. Fig. 1

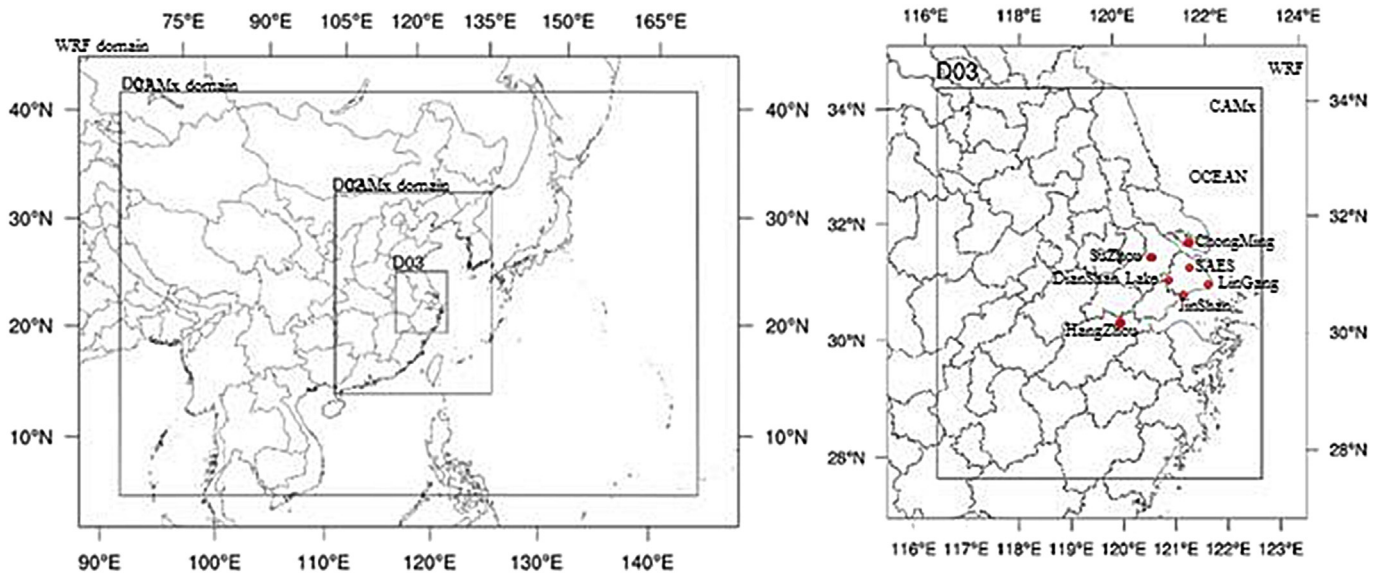

Fig. 1. One-way nested model domain (left) and the inner YRD model domain (right).

shows the source region setup. The ozone concentrations contributed by long-range transport and regional background include upwind source emissions of NOx, VOCs and other precursors transported to the YRD region which produce ozone through photochemical reactions, as well as the ozone which formed in the transportation process. Seven grids are set as receptors to analyze the ozone sources contributions, including 5 in Shanghai (Chongming, Lingang, Dianshan Lake, Jinshan, Shanghai Academy of Environmental Sciences (SAES)), 2 urban sites in Hangzhou and Suzhou, respectively, as shown in Fig. 1. The receptors of SAES, Hangzhou and Suzhou represents the sites of urban area in the YRD region; Chongming (CM) is a typical site influenced by both anthropogenic and biogenic emissions, and it is also located in the transport path between Shanghai and Jiangsu; Lingang (LG) represents a relatively clean area with small anthropogenic emissions; Jianshan (JS) is located in an industrial area with lots of volatile organic compound emissions from photochemical industry; Dianshan Lake (DSL) is also located in the transport path among Shanghai, Jiangsu and Zhejiang, but with little emissions locally.

The regional anthropogenic emission inventory in the YRD region in the year 2007 (Huang et al., 2011) are updated according to the statistical energy data of Jiangsu, Zhejiang, Anhui and Shanghai. We have developed an emission inventory of major anthropogenic air pollutants for the Yangtze River Delta region for the year 2004 (Li et al., 2011a,b) and 2007 (Huang et al., 2011), respectively. In this study, we updated the regional emission inventory to the year 2012 and added the Anhui emissions inventory for the year 2013, using the "bottom-up" methodology, same as what we used in previous studies. The emission sectors include industry, transport, residential and agriculture. The industry sector mainly include emissions from fuel combustion in power plants, boilers, kilns, and emissions directly from the industrial processes like iron and steel production, oil refining, cement production, industrial coating and printing. Transport sector include vehicle exhaust, oil evaporation, and road dust. The residential sector includes fuel combustion, domestic paint and solvent use, and gas evaporation. The agriculture sector mainly includes emissions from livestock feeding, fertilizer application and biomass burning. The emission source data are from the update of pollution source survey and the statistical data in 2012. The pollutants included in this study are SO_2, NO_x, CO, PM_{10}, $PM_{2.5}$, VOCs and NH_3.

To study the photochemical reactions of ozone, the anthropogenic VOCs emissions are speciated into its chemical species according to the CB05 mechanism based on both literature survey and on-site measurement on typical emission sources. The VOCs source profiles are based on the SPECIATE database, but we updated the profiles of vehicle exhaust, coking, solvent and biomass burning based on on-site measurement (Qiao et al., 2012; Wang et al., 2014a,b).

For biogenic VOCs (BVOCs) emissions, we updated the 2013 BVOCs emissions based on Model of Emissions of Gases and Aerosols from Nature (MEGAN Ver.2.1) (Guenther et al., 2006). Leaf area index (LAI) is from the Moderate Resolution Imaging Spectroradiometer (MODIS) product with a 1-km resolution. The plant functional type (PFT) classification scheme is used in the community land models. We also used global emission factor datasets provided along with the MEGAN2.1 model. Metrological conditions are provided by WRF modeling results. The total BVOCs emissions are then allocated to each month based on influence of meteorological conditions, as shown in Fig. 2. Compared with the isoprene (ISOP) monitoring data at SAES, the monthly profiles are reasonable and can well reproduce the temporal change. The total emissions within the YRD region has been split into 8 source categories, as shown in Table 1.

The updated regional emission inventory data are then inserted into the East Asian emission inventory provided by Multi-resolution Emission Inventory for China (MEIC) for the year 2012 developed by Tsinghua University (http://www.meicmodel.org).

The updated anthropogenic and biogenic precursor gas emissions from the 8 source categories in the YRD region are shown in Table 2.

The spatial distribution of the precursor gas emissions in the YRD region are shown in Fig. 3.

3. Model evaluation

3.1. Observed pollution episode

During July, 2013, the Yangtze River Delta region was influenced by a subtropical high pressure system. From the beginning of early July, subtropical anticyclone presenting over the YRD region and the strength of the subtropical anticyclone was strong. This

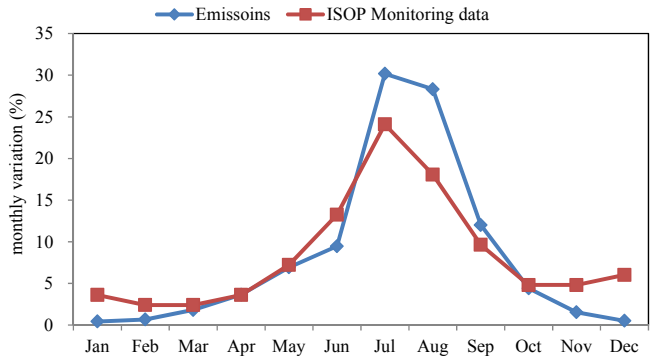

Fig. 2. Monthly profiles of BVOCs and comparison with ISOP observations at SAES.

weather pattern led to clear sunny, dry skies, with little wind, little cloud and low humidity. The solar radiation was strong, and the temperature was extremely high, reaching 41.8 °C in many cities. Fig. 4 shows the weather maps of East Asia during this period, indicating the major weather system covering the YRD region. As reported in previous studies (Li et al., 2012a, 2012b), this kind of weather system can easily cause the high ozone pollution situation.

In this period, the number of rainy days was lower compared with previous years in the YRD region and the starting date of plum rain was earlier than usual. The number of sunny days in Shanghai, Suzhou and Hangzhou in July are 11, 13 and 19, respectively, while number of cloudy days are 14, 13 and 7. The sufficient sunlight and high temperature provide favorable meteorological conditions for photochemical oxidation of ozone formation. The prevailing wind direction was southerly and the wind speed was small, creating favorable environment for the accumulation of ozone. These meteorological conditions lead to the heavy ozone pollution episode in the YRD region.

Observational data show that many cities in the YRD experienced high intensity of photochemical pollution phenomenon, showing obvious regional pollution characteristics (http://113.108.142.147:20035/emcpublish/). Fig. 5 presents the time series of the hourly averaged meteorological parameters, concentrations of ozone and NO_x in Shanghai, Suzhou and Hangzhou.

As shown in Fig. 5, two high pollution episodes are defined in the YRD region: 7 July 00:00 LST to 11 July 23:00 LST (Case I) and 20 July 0:00 LCT to 27 July 23:00 LST (Case II). In Case I, the hourly ozone concentrations range between 2.5 and 129.5 ppb (40 ppb in average). Maximum hourly ozone concentrations in Shanghai, Hangzhou and Suzhou reached 195 ppb, 138.13 ppb and 134.87 ppb, respectively. In Case II, the maximum hourly ozone concentrations in Shanghai, Hangzhou and Suzhou reached 205 ppb, 137.67 ppb and 94.73 ppb, respectively. In the following sections, we discuss the ozone source contribution regions and source categories, focusing on these two cases. Furthermore, to better understand the sources of the high level pollutants, we selected another case (00:00 LST on 13 July to 00:00 LST on 14 July; Case III) as a representative clean case, when the average concentration of O_3 were only 14.91–29.70 ppb. In Case III, the typhoon "Suli" affected eastern China, causing better meteorological conditions for dispersion.

3.2. Comparison of model results and observations

Based on the data availability, the model predicted ozone concentrations at 4 sites are compared with the observational data, including urban Shanghai (SAES), Hangzhou, Suzhou and Dianshan Lake. Locations of the monitoring sites are shown in Fig 8. Fig. 6 shows the time variations of the model predicted and observed hourly averaged ozone concentrations at 4 monitoring sites. As shown in the figures, the WRF-CAMx modeling system reproduces the ozone variation trends in different areas in the YRD region very well.

Statistical methods used to do model verification include the Bias, Normalized Mean Bias (NMB), Normalized Mean Error (NME) and Index of Agreement (IOA) (Boylan and Russell, 2006), which have been widely used in air quality modeling research. Table 3 shows the statistical results of the predicted and observed hourly

Table 1
Split of the emission categories.

Source categories	Contents	Major O_3 precursors
Power plants	Coal burning, gas burning power plants	NOx、CO
Industrial boiler and kilns	Coal, heavy oil, coke, gas burning and other industrial boilers and furnaces	NOx、VOCs、CO
Industrial process	Petrochemical and chemical industry, cement production, steel, coke and other processes	VOCs、NOx
Mobile source	Gasoline vehicle exhaust, diesel vehicle exhaust, evaporative emissions, ships, aircrafts	NOx、VOCs
Volatile source	Coating, volatile oil and gas, food fumes	VOCs
Residential	Domestic fuel consumption	NOx、VOCs
Agricultural source	Biomass burning	VOCs
Biogenic emission	Plants	VOCs

Table 2
Precursor gas emissions in the YRD region in 2012 (BVOCs are for the year 2013).

	NOx, kt/year				VOCs, kt/year			
	Shanghai (2012)	Jiangsu (2012)	Zhejiang (2012)	Anhui (2013)	Shanghai (2012)	Jiangsu (2012)	Zhejiang (2012)	Anhui (2013)
Power Plants	80.7	542.9	344.5	57.8	1.3	5.1	6.9	0.5
Industrial boiler and kilns	104.0	631.8	439.2	309.0	50.1	43.0	64.1	13.1
Industrial process	4.1	14.2	6.5	9.4	327.3	884.3	678.1	169.5
Mobile	82.2	231.1	158.6	144.8	60.6	399.6	301.5	76.1
Volatile	–	–	–	–	62.5	296.8	244.9	125.9
Residential	5.8	4.0	5.7	8.9	4.5	11.4	7.7	5.6
Agricultural	0.1	33.2	8.0	32.3	0.8	189.1	45.6	183.9
Biogenic					29.1	472.5	1174.6	905.2
Total	**276.9**	**1457.3**	**962.6**	**562.3**	**536.1**	**2301.9**	**2523.5**	**1479.9**

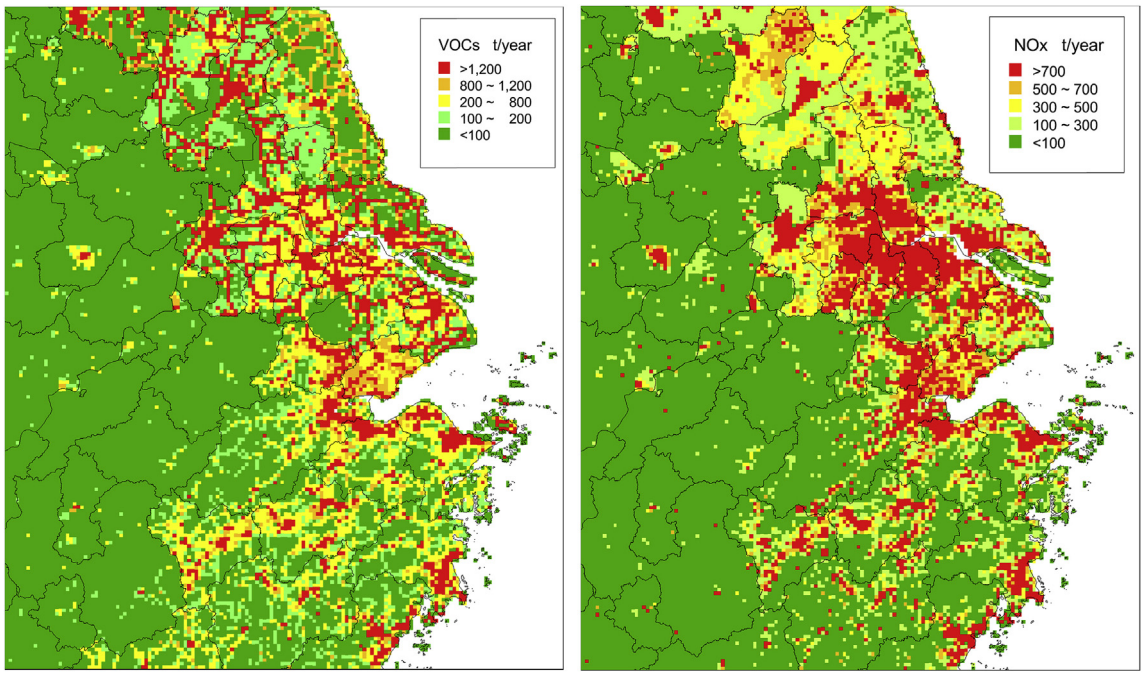

Fig. 3. Spatial distribution of the ozone precursor gas emissions at the surface layer in YRD.

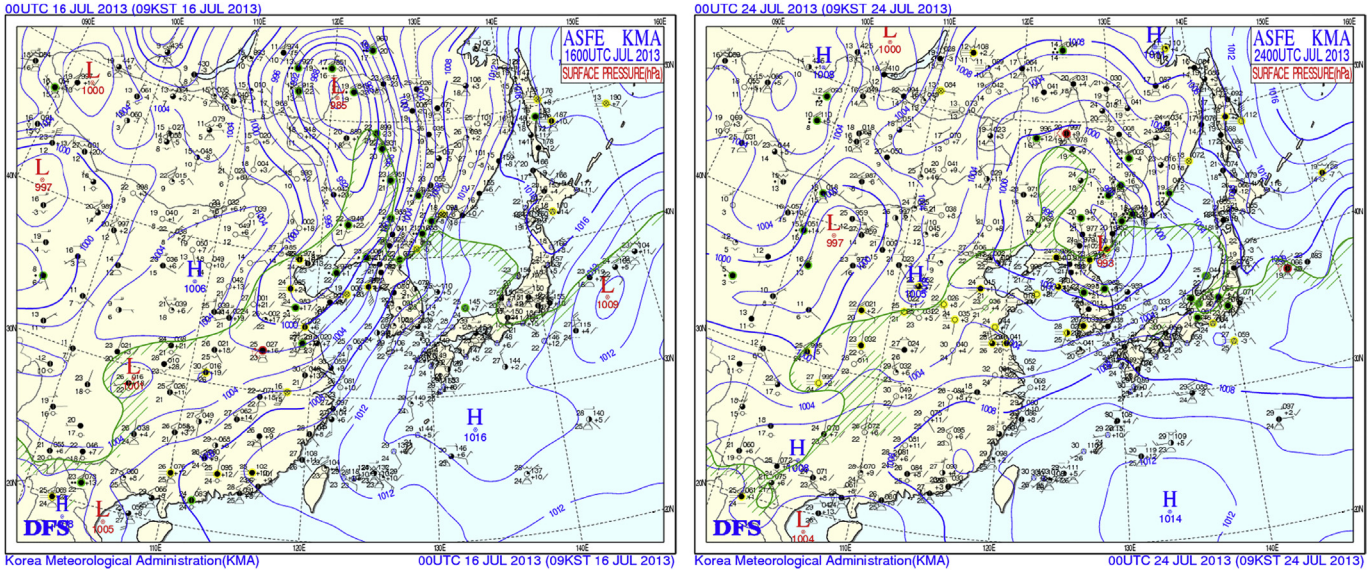

Fig. 4. Weather patterns over the eastern Asia during on July16 and 24, 2013.

O_3 concentrations. The modeled hourly average, the maximum and minimum O_3 concentrations are all close to the observed data. Results show that CAMx can reproduce the variation trends of the O_3. The index of agreement for O_3 at the 4 monitoring sites ranges between 0.81 and 0.88, as shown in Table 3a, statistical results between model predicted and observed NO_2 are also shown in Table 3b, indicating that the model captures well the diurnal variations of the pollutants (see Fig. 6).

There are some bias between the model predicted and observed O_3 concentrations, ranging between −0.29–0.51. The bias between the model predicted and observed NO_2 concentrations, ranging between −0.38–1.00. These biases are mainly due to the uncertainties in local and regional emission inventory, meteorology, and deviation of observations, which may affect source apportionment results to some extent. However, the general model performance indicates that the WRF-CAMx modeling system has reproduced the pollution episode, the temporal and spatial characteristics of ozone in the YRD region. Thus, the modeling system is acceptable to do source apportionment, which can provide valuable insights into the major source regions and source categories that control high O_3 concentrations.

The model bias of O_3 and NO_2 simulations can be attributed to the uncertainties in emissions, meteorology, and deviation of observations. These model biases may affect ozone source apportionment results to some extent. For example, over-prediction of NO may cause some of the over titration of the O_3 by

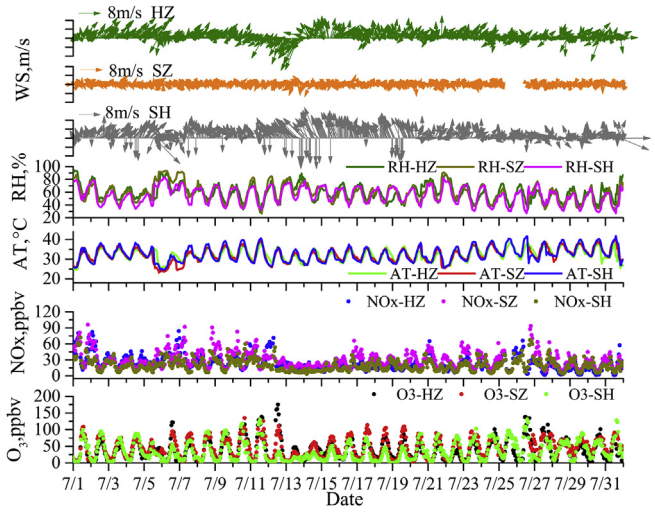

Fig. 5. Time series of the hourly averaged meteorological parameters, O_3 and NO_x concentrations in Shanghai, Hangzhou and Suzhou in July, 2013. (SH: Shanghai; HZ: Hangzhou; SZ: Suzhou).

photochemistry. The over-prediction of wind speed may cause the over-prediction of regional contribution to O_3 from regional and super-region. And the error of simulated temperature may also affect the photochemical of O_3. There is also a kind of uncertainty on the estimation of the contributions from long-range transport. In this paper, we defined boundary conditions as LRT. However, regional emissions can be transported out of the domain and then re-imported into the domain which is defined as BCs. Thus, the contribution from LRT may be overestimated to some extent. Nevertheless, the model performance shows that the WRF-CMAQ performance are acceptable compared to related studies (Liu et al., 2010; Wang et al., 2010). Thus, the modeling system can be used to do source apportionment to provide valuable insights into the governing processes that control O_3 concentrations (see Tables 4 and 5).

4. Results and discussion

4.1. Separation of ozone formation under NOx- or VOC-limited conditions

The OSAT methodology coupled within CAMx use reactive tracers to represent VOCs and NOx emissions from the assigned 8 source groups. At each time step and each receptor, ozone formation from VOCs and NOx precursors is tracked separately. The ozone reactive tracer associated with each source group is then transported, dispersed, deposited and chemical destroyed following the processes in CAMx. Fig. 6 differentiate the NOx- and VOC-limited ozone formation at the different receptors in YRD region in July, 2013.

As shown from Fig. 7, the ozone formation in the YRD region is mostly under VOC-limited situation, with VOCs contribution (O_3V tracers) to total ozone (O_3T) ranging between 47 and 71%. At urban Shanghai, Hangzhou and Suzhou receptors, the O_3V contribution accounts for 57%, 47% and 53%, respectively. This result indicates that in urban area of the YRD, reducing local and upwind VOCs emissions are useful to reduce ozone concentrations. At suburban area like Jinshan and Lingang, the O_3V contributions to total O_3 are 53% and 55%, showing that rural ozone is also sensitive to VOCs emissions. At Chongming site, the O_3V contribution is as high as 71%, due to the rich biogenic emissions in this area. In comparison,

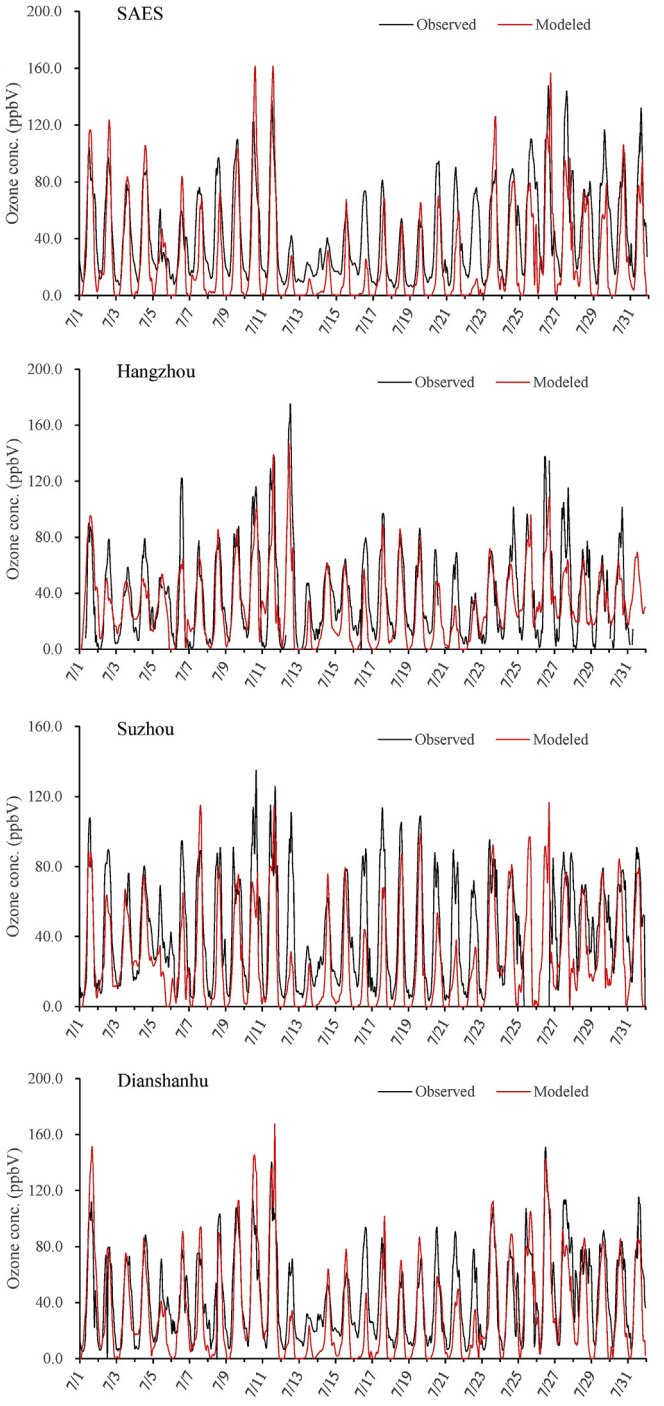

Fig. 6. Time series of the model predicted and observed ozone concentrations during July, 2013.

at the junction area (Dianshan Lake), O_3V and O_3N plays almost the same role in ozone formation, with the contribution of 51% and 49%, showing that reducing VOCs and NOx can obviously reduce ozone in this area.

4.2. Spatial distribution of ozone regional contribution

The model predicted regional contribution to daytime 8-h (9:00–17:00) O_3 and daily max O_3 at the main receptors in the YRD are shown in Fig. 8. At all sites, high ozone concentrations were

Table 3a
Statistical results between model predicted and observed O_3 during July, 2013.

	Number of data pairs	Hourly average, ppbV		Max, ppbV		Min, ppbV		NMB (%)	NME (%)	IOA	Bias	Correlation coefficient
		Modeled	Observed	Modeled	Observed	Modeled	Observed					
SAES	743	26.43	42.45	161.61	147.57	0.00	5.60	−37.73	47.80	0.84	−0.53	0.80
Hangzhou	683	31.52	38.67	147.00	175.00	0.00	0.47	−18.51	39.76	0.86	0.51	0.79
Suzhou	709	26.25	43.21	114.95	134.96	0.00	3.27	−39.24	44.24	0.81	−0.45	0.78
Dianshan Lake	742	33.48	43.71	167.48	150.84	0.00	5.14	−23.39	39.49	0.88	−0.29	0.83

Table 3b
Statistical results between model predicted and observed NO_2 during July, 2013.

	Number of data pairs	Hourly average, ppbV		Max, ppbV		Min, ppbV		NMB (%)	NME (%)	IOA	Bias	Correlation coefficient
		Modeled	Observed	Modeled	Observed	Modeled	Observed					
SAES	733	17.08	15.98	64.90	61.77	0.65	2.56	6.88	50.47	0.65	0.19	0.45
Dianshan Lake	733	23.60	14.96	84.20	62.82	1.06	0.49	57.75	82.47	0.56	1.00	0.47
Suzhou	703	19.20	17.45	77.69	59.41	1.35	4.38	9.79	52.25	0.70	0.09	0.60
Hangzhou	712	11.63	19.87	96.89	63.79	1.38	1.46	−41.48	57.49	0.62	−0.38	0.46

Table 4
Source category contribution to daytime 8-h O_3 in YRD during July, 2013.

		Agriculture	Industrial boilers and kins	Industrial processing	Traffic	Power plants	Residential	Volatile	Biogenic	LRT
Urban	Shanghai	0.0%	16.3%	12.6%	15.2%	3.7%	0.3%	3.8%	23.1%	24.9%
	Hangzhou	0.0%	3.3%	21.4%	14.6%	3.8%	0.2%	1.6%	18.6%	36.4%
	Suzhou	0.1%	7.6%	16.9%	11.4%	3.6%	0.1%	2.5%	23.6%	34.1%
Rural	Chongming	0.1%	26.7%	7.4%	14.4%	3.8%	0.1%	5.1%	24.0%	18.5%
	Lingang	0.0%	16.8%	10.5%	12.2%	6.4%	0.2%	4.5%	24.9%	24.4%
	Jinshan	0.1%	11.7%	15.8%	13.8%	5.1%	0.2%	3.7%	24.6%	25.1%
Conjunction	Dianshan Lake	0.1%	10.6%	18.0%	14.5%	4.0%	0.2%	3.2%	23.9%	25.5%

Table 5
Source category contribution to daily max O_3 in YRD during July, 2013.

		Agriculture	Industrial boilers and kins	Industrial processing	Traffic	Power plants	Residential	Volatile	Biogenic	LRT
Urban	Shanghai	0.0%	20.2%	14.9%	15.2%	4.4%	0.3%	3.9%	22.4%	18.8%
	Hangzhou	0.0%	3.8%	24.3%	15.7%	5.7%	0.2%	2.0%	17.6%	30.7%
	Suzhou	0.1%	9.1%	20.8%	13.2%	4.8%	0.1%	2.7%	22.2%	27.0%
Rural	Chongming	0.1%	30.0%	9.8%	14.7%	4.9%	0.1%	4.7%	21.3%	14.5%
	Lingang	0.0%	20.4%	13.3%	12.8%	7.5%	0.2%	3.8%	23.0%	18.9%
	Jinshan	0.0%	13.3%	19.5%	13.7%	6.5%	0.2%	3.3%	23.4%	20.0%
Conjunction	Dianshan Lake	0.1%	12.1%	20.6%	14.8%	5.3%	0.2%	3.2%	22.9%	20.9%

caused by combined effect of local, regional photochemical reactions and long-range transport. However, there are some differences among the receptors at different locations. In summer, the prevailing wind direction in YRD is southerly, therefore, contributions from Zhejiang is obvious to all receptors. At urban Hangzhou, around 60% of ozone mass concentrations are formed due to precursor emissions in Zhejiang province, with another 40% coming from other areas and the south boundary. Jinshan is located close to Zhejiang boundary; it is highly affected by precursor emissions in Zhejiang, which accounts for half of the ozone concentrations. At the urban Shanghai, besides significant contributions from upwind precursor emissions in Zhejiang province (36%), local emissions also contribute significantly to 8-h ozone formation, with the percentage of 17.6%, emissions from Anhui account for 15.3%, outside domain accounts for 24.9%.

Dianshan Lake (DSL) is located at the junction of two provinces and Shanghai city. It is influenced by all the three areas and the long-range transport. As shown from the figure, the daily max O_3 at the DSL are contributed by Zhejiang (48.5%), Jiangsu (11.7%), Anhui (11.6%) and Shanghai (7.4%), long-range transport constitutes around 20.9% of the daily max O_3 in July.

Chongming (CM) is located at the pollution transport channel between Shanghai and Jiangsu. The modeling results indicate that Shanghai constitutes 15.6% of the daily max O_3, Jiangsu contributes 16.2%, Anhui contributes 28.2% and Zhejiang accounts for 25.5%. The peak ozone is more influenced by local photochemistry, with 15.6% from Shanghai, higher than the contribution to 8-h average (12.8%).

The high O_3 at the Lingang (LG) receptor mainly comes from the photochemical reactions among precursor gases in Zhejiang, Anhui, Shanghai, and long-range transport, with the contribution to daily max O_3 of 39.6%, 39.1%, 2.2%, 18.9%, respectively.

At most receptors, the contribution from local chemistry to peak ozone is higher than 8-h average, indicating that although upwind region and long-range transport dominate mean ozone conditions, elevated local sources are the contributing factor for formation of high ozone concentrations.

4.3. Temporal change of the ozone regional contribution

Regional contribution to hourly averaged O_3 at receptors of the YRD region changes quite a lot under influence of meteorological

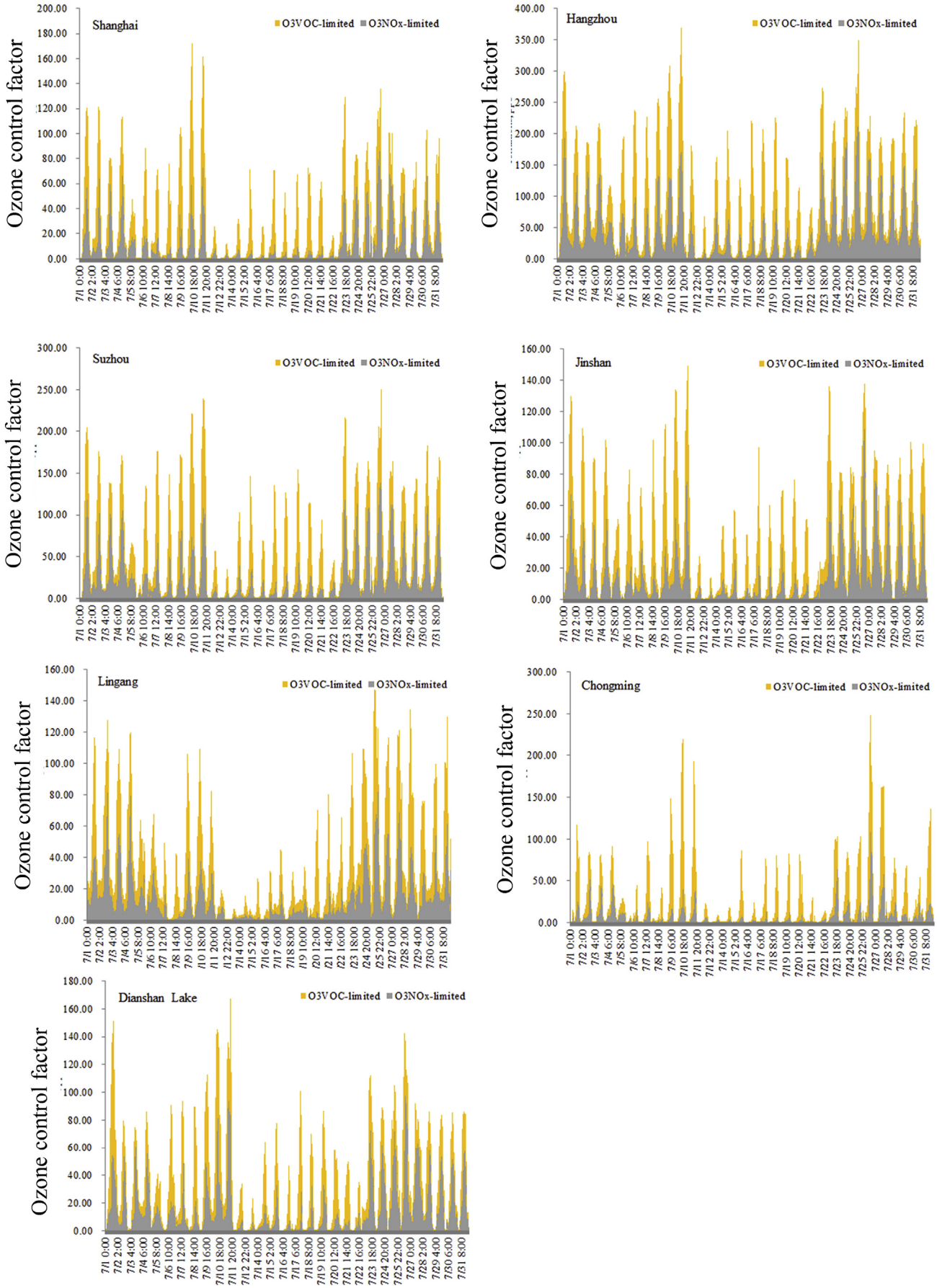

Fig. 7. Separation of ozone formation under NOx- or VOC-limited conditions in the YRD in July, 2013.

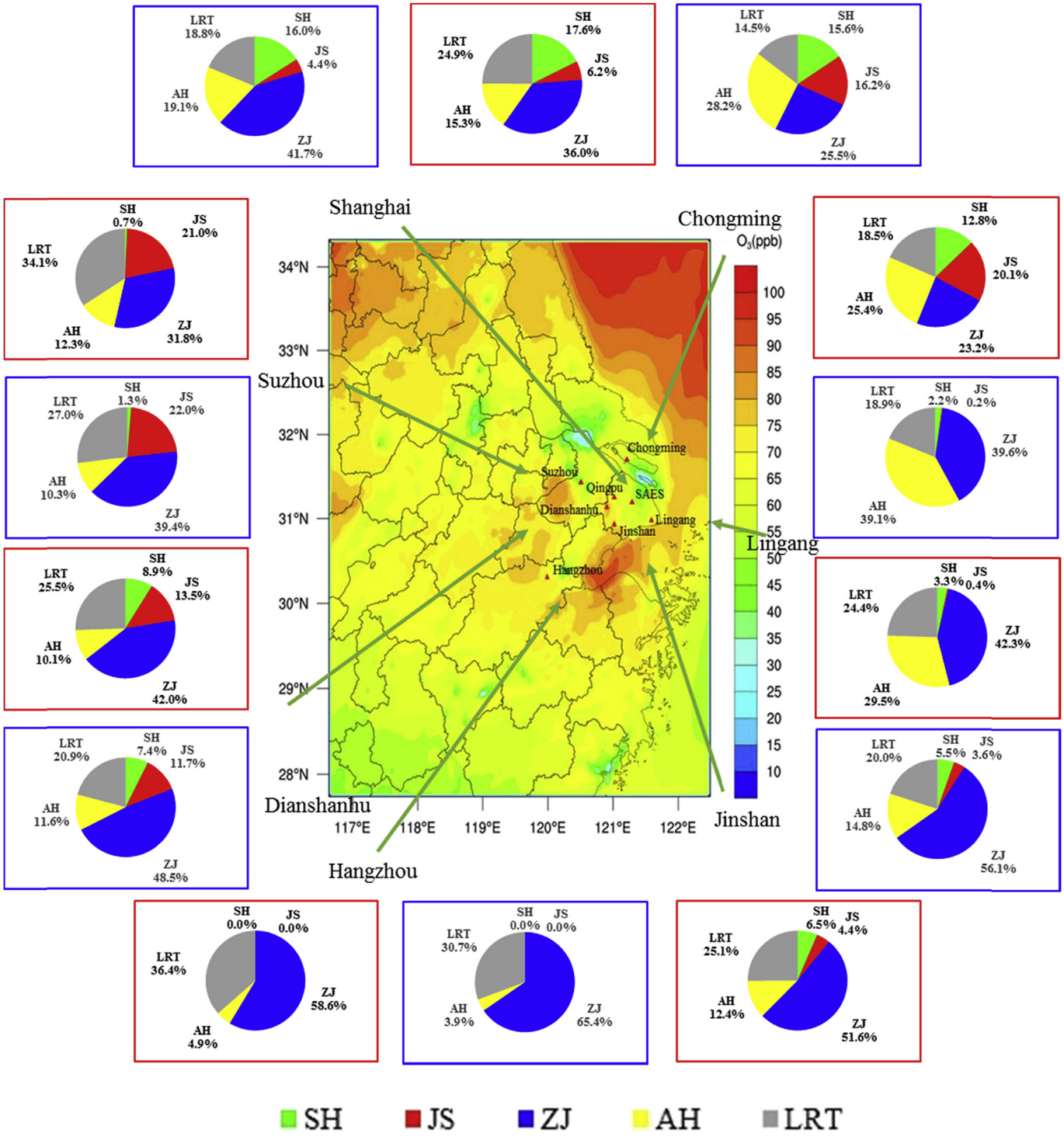

Fig. 8. Regional contribution to daytime 8-h O_3 (Red box) and daily max O_3 (Blue box) in the YRD in July, 2013 (SH: Shanghai; JS: Jiangsu; ZJ: Zhejiang; AH: Anhui; LRT: Long-range transport).

conditions, as shown in Fig. 9. Long-range transport is the dominant factor at night time and to rural area close to the ocean (at receptors like Lingang). In comparison, local emissions play a more significant role in daytime and to formation of hourly max O_3 concentrations.

Among all receptors setup in the modeling system, Shanghai, Hangzhou and Suzhou represents urban area, indicating high NOx emission rates with large vehicle population, and relatively rare industries with VOCs emissions around. Results show that in urban area, long-rang transport causes around 20–40 ppb of O_3 on average. However, for high hourly O_3 concentrations at the urban receptors, contributions from local emissions increase significantly. The contributions to hourly O_3 at SAES site from Shanghai is up to 74.06%, together with contributions from Zhejiang, Anhui and Jiang, causing high ozone peaks in daytime. Suzhou is similar to urban Shanghai, ozone concentrations can reach very high under

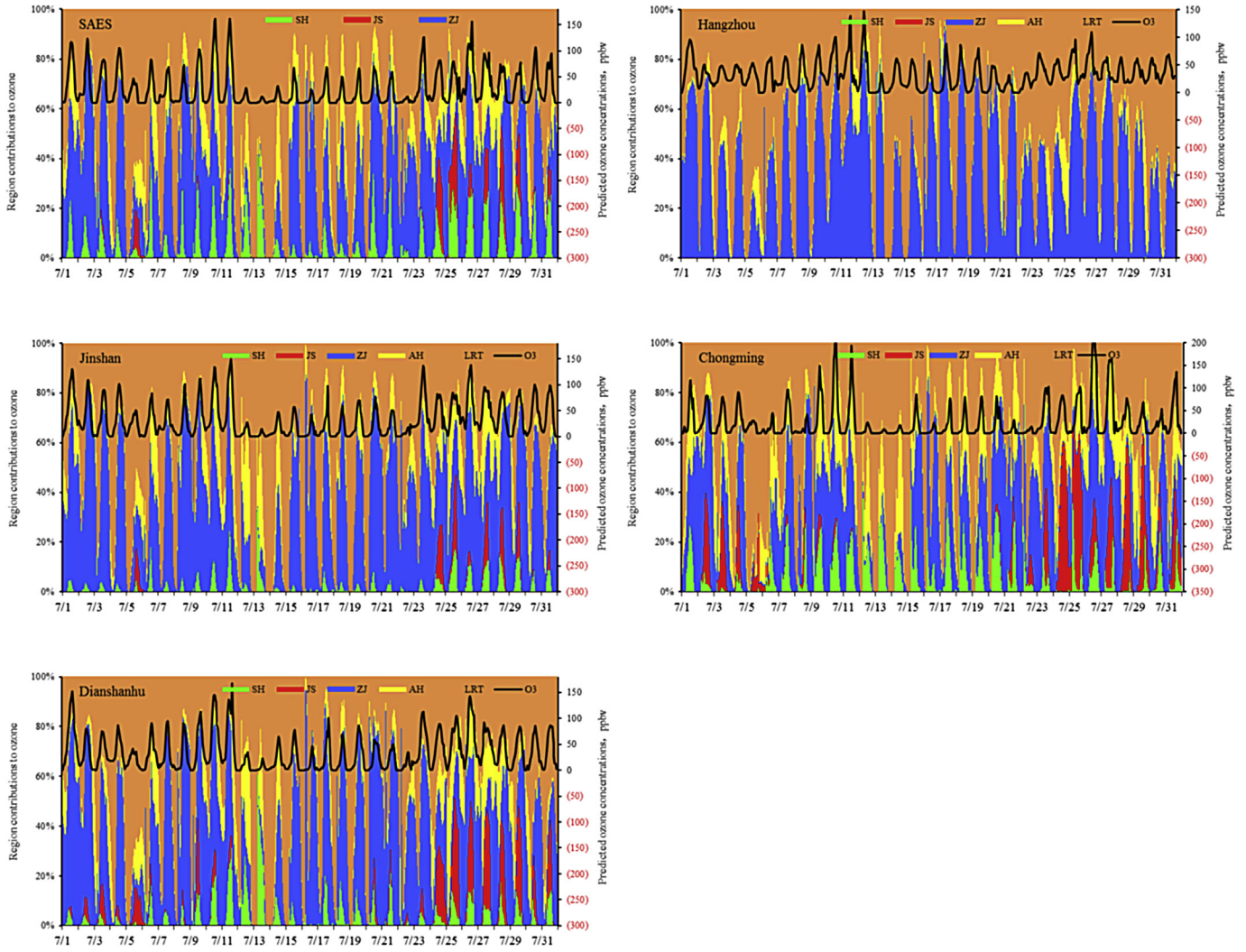

Fig. 9. Time series of the regional contribution to hourly O_3 concentrations during July, 2013.

influence from all the three regions. Hangzhou is located in the southwest of the Yangtze River Delta modeling domain, and it is the upwind region of both Shanghai and Jiangsu province. Regional contributions to Hangzhou O_3 are different from Shanghai and Suzhou. The daily high ozone concentrations in this period are mainly from local source photochemical reaction and long-range transport.

For Jinshan, Lingang, Chongming and Dianshan Lake, their ozone concentrations are mainly controlled by Zhejiang. However, the ozone reached much higher concentrations from July 25, due to contributions from Shanghai and the three provinces, showing that the western and southwestern wind may increase ozone in the whole region.

4.4. Regional contribution in different pollution episodes

Two high pollution episodes occurred during July, 2013. Case I was from 7 July 00:00 LST to 11 July 23:00 LST. During this period, the maximum hourly ozone concentration in Shanghai reached 161.61 ppb. The maximum solar radiation was 915.2 W/m^2, the average wind speed was only 1.7 m/s in urban Shanghai area, and 4.6 m/s at the Hongqiao airport; the prevailing wind direction was southerly. Fig. 10 shows the average wind field and distribution of average daily maximum O_3 during this episode. Daily max O_3 contributions include 23%–61% from long-range transport and regional background. Regional contributions from YRD vary with locations of the receptors. At SAES site, 14.1% ± 14.5%,46.9% ± 16.5% O_3 is contributed by Shanghai and Zhejiang province, respectively. At the CM receptor, 21.6% ± 10.5% O_3 is caused due to precursor emissions in the Shanghai area. At DSL site, Zhejiang contributes 62.0% ± 18.3% O_3. For this result, it is quite obvious that the precursor gas emissions in both Zhejiang and Shanghai regions cause high ozone pollution episode in the downwind area of the YRD region.

Case II was from 20 July 0:00 LST to 27 July 23:00 LST. During this period, the solar radiation was 909.5 W/m^2, the average wind speed was 1.6 m/s in urban Shanghai area, and 3.9 m/s at the Hongqiao airport; the prevailing wind direction was southwestly. Fig. 11 shows the average wind field and distribution of average daily maximum O_3 during this episode. During Case II, the long-range transport contribution to daily max O_3 at SAES, SZ, HZ increased to 22.45%, 31.25% and 34.57% in average. Besides, Shanghai and Zhejiang have significant impact on maximum O_3 at SAES, LG, and CM, while Jiangsu and Zhejiang are more important to DSL.

In Case III, since the typhoon “Suli” affected eastern China, causing high wind speed (4.2 m/s in urban Shanghai and 8.2 m/s at the HongQiao airport in average), the O_3 concentrations were

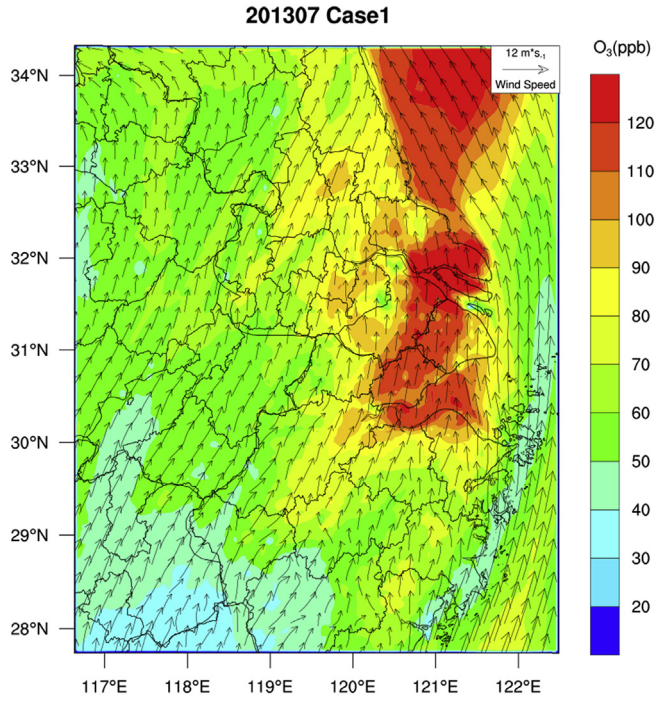

Fig. 10. Hourly averaged wind pattern and distribution of average daily maximum O_3 during Jul.7–11, 2013.

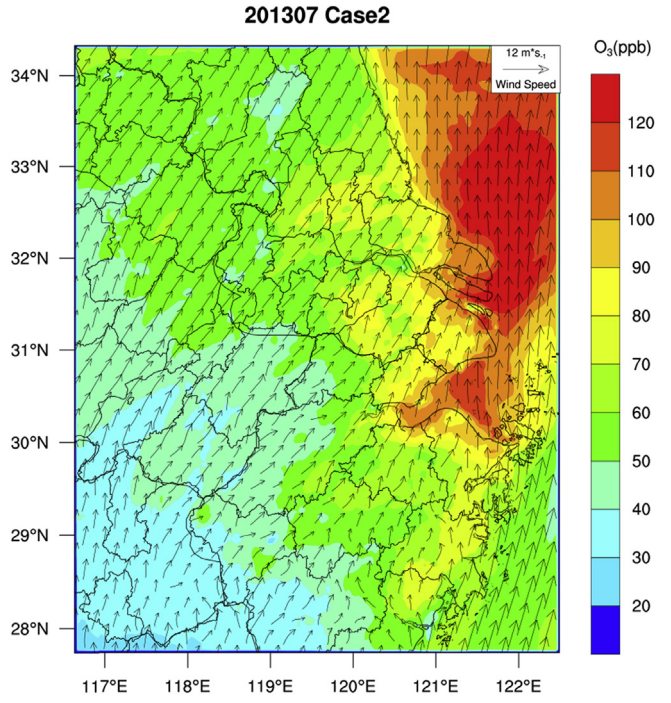

Fig. 11. Hourly averaged wind pattern and distribution of average daily maximum O_3 during Jul.20–27, 2013.

relatively low, with most coming from long-range transport and regional background (referring to initial and boundary conditions of O_3) at the sites of SAES, HZ, SZ, JS and LG. However, Shanghai is the most important region contributing to O_3 at CM and DSL. Fig. 12 shows the wind pattern and distribution of average daily maximum

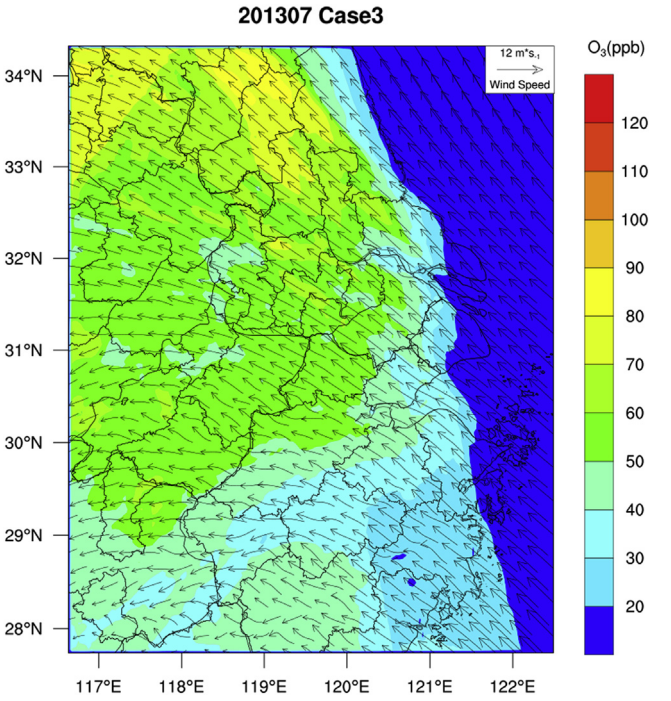

Fig. 12. Hourly averaged wind pattern and the distribution of average daily maximum O_3 during Jul.13–14, 2013.

O_3 during this episode.

4.5. Spatial distribution of ozone source category contribution

Besides the regional contribution to surface ozone, the ozone source apportionment in terms of source sectors is also very important, since the pollution control strategy is usually developed based on the anthropogenic emission source categories. The model predicted source category contributions to daytime 8-h (9:00–17:00) O_3 and daily max O_3 at the main receptors in YRD are shown in Fig. 13. The major source categories contributing to high O_3 in the YRD region includes industrial boilers and kilns (up to 30.0%) from fuel combustion, industrial processing (up to 24.3%), transportation (up to 15.7%), and biogenic emissions (up to 24.9%). Power plants cannot be negligible, which have a significant contribution to downwind rural areas. For peak ozone at LG and JS, power plans contribute 7.5% and 6.5% of ozone formation in average.

4.6. Temporal change of ozone source contribution

Fig. 14 shows the main source category contributions to hourly O_3 in the YRD region in July 2013. In terms of the sources to the summer time photochemical pollution, the major sectors include industrial production process, industrial boilers and furnaces, mobile sources, and biogenic emissions. Crude oil processing, chemicals, building materials and the production and use of industrial solvents in the production process discharge a lot of volatile organic compounds (VOCs), fuels coal, heavy oil, coke from industrial boilers and furnaces discharge a lot of NOx. The exhaust of motor vehicle includes VOCs and NO_x. Therefore, precursor emission sources in the Yangtze River Delta region contribute to the high concentrations of urban O_3.

Modeling results indicate that ozone contributions from industrial production process to Shanghai, Suzhou and Hangzhou are

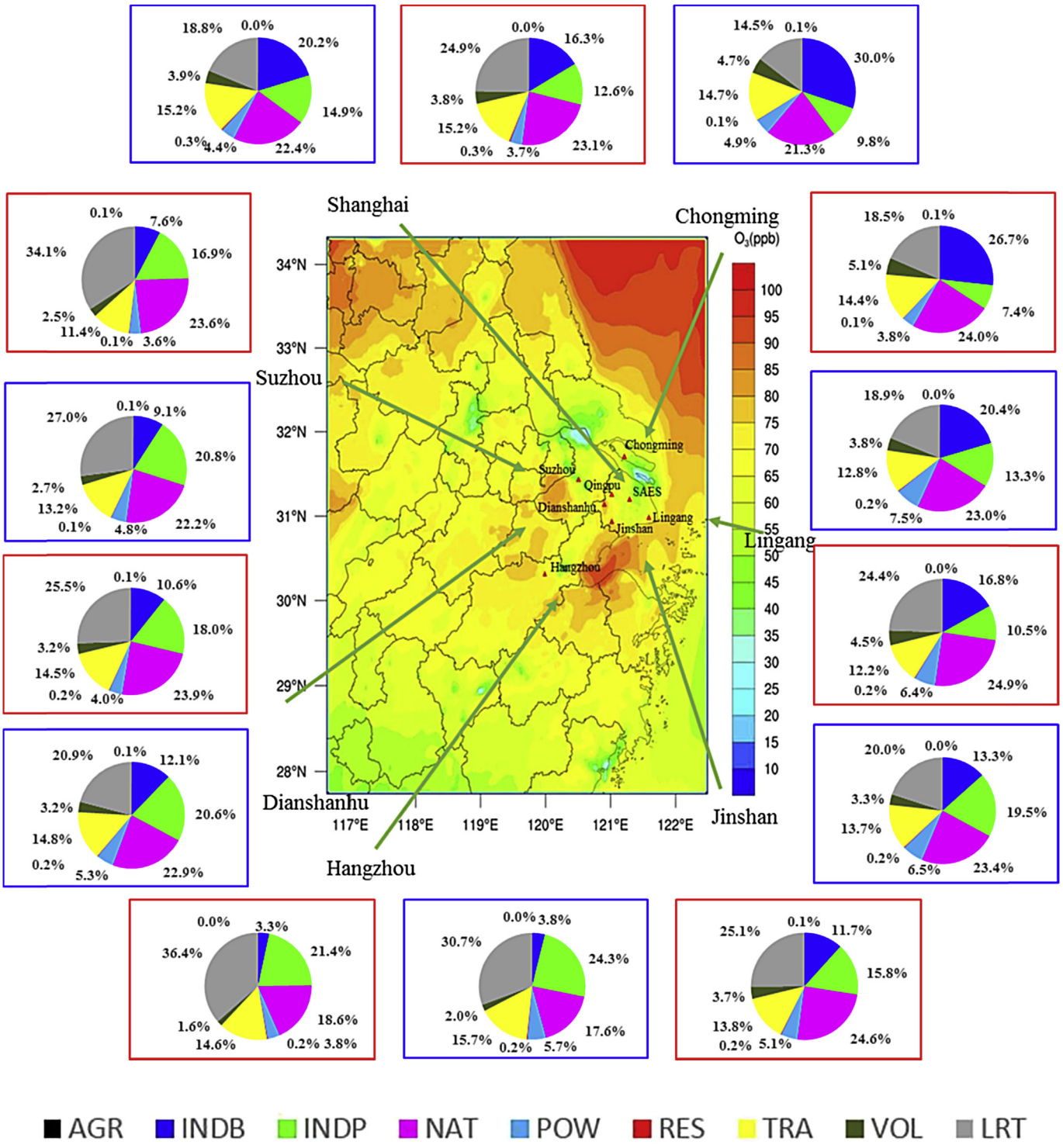

Fig. 13. Source category contribution to daytime 8-h O_3 (Red box) and daily max O_3(Blue box) in the YRD in July, 2013 (AGR: agriculture; INDB: industrial boilers; INDP: industrial processing; NAT: biogenic; POW: power plants; RES: residential; TRA: transport; VOL: volatile emissions; LRT: long range transport).

14.9%, 20.8%, and 24.3%, respectively. Fuel combustion from industrial boilers and kilns account for 20.2%, 9.1%, and 3.8%, respectively. Mobile sources including vehicle exhaust, ship emissions and non-road are also significant, with the average contribution reaching15.2%, 13.2%, and 15.7%, respectively. The source category contributions to O_3 at rural sites are similar. The contributions to hourly O_3 at CM site from mobile source, industrial processing, volatile source, biogenic emissions, industrial boilers and kilns, power plants and residential range between 0.00% and 25.8%, 0.0%–40.6%, 0.0%–26.3%, 0.0%–54.8%, 0.0%–57.2%, 0.0%–18.8%, 0.0%–1.0%, respectively.

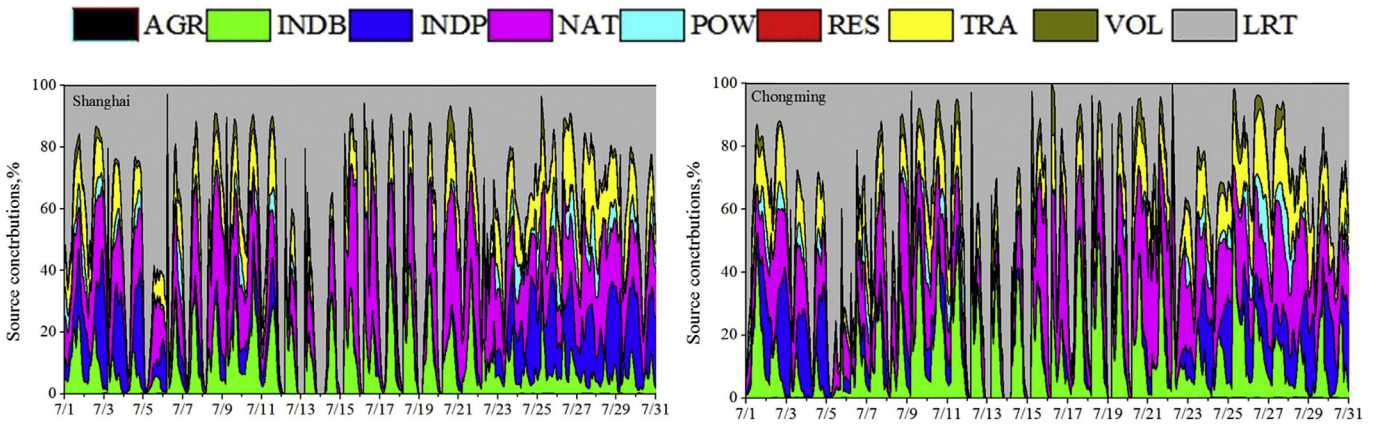

Fig. 14. Time series of the source category contribution to hourly O_3 concentrations during July, 2013 (AGR: Agriculture; INDB: Industrial boilers; INDP: Industrial Processing; NAT: Natural source; POW: Power plants; RES: Residential; TRA: Traffic; VOL: Volatile evaporation source; LRT: Long-range transport).

4.7. Source category contribution to ozone in different pollution cases

During Case I and Case II, the temperature is high, and the wind speed is low. Under this favorable meteorological conditions, the transportation impact is very obvious in most receptors, accounting for 11.0–14.3% of daytime 8-h O_3 at different receptors in average. Industry is the second significant source category that influences high O_3 in case I, among which, industrial processing contributes 4.3–22.2% of daytime 8-h O_3 in average, and industrial boilers and kilns accounting for 3.3–31.1%.(During Case I and Case II, biogenic emissions impact is very obvious in most receptors, accounting for 20.0–30.0% of daytime 8-h O_3 at different receptors in average.

There is not so much difference between Case I and Case II in terms of the source category contribution. However, Case III is different due to the changed weather system. At SAES, JS and LG site, the contributions from all the anthropogenic emissions are smaller than the other two pollution cases due to increase of the long-range transport. At the SZ, HZ, JS and DSL site, the day time 8-h O_3 contribution from industrial boilers and kilns and biogenic emissions increased significantly. At SZ site, the industrial boilers and kilns contribution increased from 7.5% in Case I and 4.2% in Case II to 21.1% in Case III, and the biogenic contribution decreased from 28.0% in Case I and 25.4% in Case II to 22.9% in Case III. At HZ site, the industry contribution increased from 3.3% in Case I and 1.2% in Case II to 10.9% in Case III, the biogenic contribution decreased from 26.7% in Case I to 25.2% in Case III. At JS site, the industrial boilers and kilns increased from 16.1% in Case I and 7.9% in Case II to 20.3% in Case III, the biogenic contribution decreased from 29.5% in Case I and 25.6% in Case II to 18.4% in Case III. At DSL site, the industrial boilers and kilns increased from 12.9% in Case I and 7.9% in Case II to 24.0% in Case III, the biogenic contribution decreased from 27.8% in Case I and 27.0% in Case II to 23.5% in Case III.

5. Conclusions

This paper selects a summer time photochemical pollution period to do a case study with the application of OSAT coupled within the CAMx air quality model. The contributions from regions and source categories to high ozone at 7 receptors in the YRD region are analyzed. During the summer high ozone pollution period in July 2013, long-range transport and regional background dominates the night-time ozone in the YRD region. The daytime ozone in the surface atmosphere is formed through complex photochemical reactions following emissions of precursor gases such as NO_x and VOCs under presence of the sunlight. The daytime ozone concentrations in the YRD region are influenced by emissions both locally, regionally and in other areas outside the YRD region. At the junction among two provinces and Shanghai city, ozone is usually influenced by all the three areas and the long-range transport outside the modeling domain. The daily max O_3 at the DSL are contributed by Zhejiang (48.5%), Jiangsu (11.7%), Anhui (11.6%) and Shanghai (7.4%), long-range transport constitutes around 32.5% of the daily max O_3 in July. At the Chongming (CM) site, Shanghai constitutes 15.6%, Jiangsu contributes16.2%, Anhui contributes and Zhejiang accounts for 25.5% of the daily max O_3. In comparison, at the urban Shanghai (SAES) area, 16.0% O_3 are influence by local Shanghai, 41.7% from Zhejiang and 4.4% from Jiangsu region.

The analysis of the source category contribution to high ozone in the Yangtze River Delta region indicates that the most prominent types of emission sources contributing to O_3 pollution include industrial boilers and kilns, industrial production process, and mobile source. Emissions of NO_x and other precursors emitted from the fuel combustion of industrial boilers and kilns contribute a lot to the high concentration in Hangzhou and Suzhou, while various volatile organic compounds discharged from industrial production process contributed a lot to the ozone in Shanghai. The contribution from vehicle exhaust in the whole region can reach 15.7%. The contribution from regional elevated power plants cannot be neglected, especially to rural area. Unorganized VOCs emissions of volatile evaporation pollution sources also have certain contribution to regional concentration of O_3. Therefore, the emissions from fuel combustion, VOCs emissions from industry and vehicle exhaust are the main anthropogenic sources causing high ozone concentrations in the Yangtze River Delta region.

This research shows that the O_3 pollution in Shanghai, Jiangsu and Zhejiang is caused by the joint effect from precursor emissions within local, regional and even super-regional area. The high O_3 episode in the YRD region, especially in the downwind area, is mainly attributed by different source regions and major anthropogenic source categories including industry and vehicle exhaust. These results indicate that the regional collaboration is of most importance to reduce ambient ozone pollution, particularly during high ozone episodes. Results also show that the ozone formation at most receptors especially in urban area are under VOC-limited situation, therefore, the regional control on reactive VOCs are of great significance to control ozone pollution situation.

Acknowledgements

This study was financially supported by the “Chinese National

Key Technology R&D Program" via grant No. 2014BAC22B03, the "Chinese National Non-profit Scientific Research Program" via grant No. 201409008, the National Natural Science Foundation of China via grant No. 41205122, and the Key research project related to ozone formation from Shanghai Environmental Protection Bureau. All observational and modeling data used in this paper can be obtained on request by emailing the author.

References

Boylan, W.J., Russell, A.G., 2006. PM and light extinction model performance metrics, goals, and criteria for three-dimensional air quality models. Atmos. Environ. 40, 4946–4959.

Byun, D., Schere, K.L., 2006. Review of the governing equations, computational algorithms, and other components of the Models-3 Community Multiscale Air Quality (CMAQ) modeling system. Appl. Mech. Rev. 59, 51–77.

Chen, P.F., Quan, J.N., Zhang, Q., Tie, X.X., Zhang, Q., Gao, Y., Li, X., Huang, M.Y., 2013. Measurements of vertical and horizontal distributions of ozone over Beijing from 2007 to 2010. Atmos. Environ. 74, 37–44.

Ding, A.J., Fu, C.B., Yang, X.Q., Sun, J.N., Zheng, L.F., Xie, Y.N., Herrmann, E., Petäjä, T., Kerminen, V.M., 2013. Ozone and fine particle in the western Yangtze River Delta: an overview of 1 yr data at the SORPES station. Atmos. Chem. Phys. 13, 5813–5830.

ENVIRON, 2015. CAMx User's Guide Comprehensive Air Quality Model with Extensions Version 6.2. ENVIRON International Corporation.

Feng, Z.Z., Sun, J.S., Wan, W.X., Hu, E.Z., Calatayud, V., 2014. Evidence of widespread ozone-induced visible injury on plants in Beijing, China. Environ. Pollut. 193, 296–301.

Foley, K.M., Roselle, S.J., Appel, K.W., Bhave, P.V., Pleim, J.E., Otte, T.L., Mathur, R., Sarwar, G., Young, J.O., Gilliam, R.C., Nolte, C.G., Kelly, J.T., Gilliland, A.B., Bash, J.O., 2010. Incremental testing of the community multiscale air quality (CMAQ) modeling system version 4.7. Geosci. Model Dev. 3, 205–226. http://dx.doi.org/10.5194/gmd-3-205-2010.

Fu, X., Wang, S.X., Zhao, B., Xing, J., Cheng, Z., Liu, H., Hao, J.M., 2013. Emission inventory of primary pollutants and chemical speciation in 2010 for the Yangtze River Delta region, China. Atmos. Environ. 70, 39–50.

Geng, F.H., Zhao, C.S., Tang, X., Lu, G.L., Tie, X.X., 2007. Analysis of ozone and VOCs measured in Shanghai: a case study. Atmos. Environ. 41, 989–1001.

Gery, M.W., Whitten, G.Z., Killus, J.P., Dodge, M.C., 1989. A photochemical kinetics mechanism for urban and regional scale computer modeling. J. Geophys. Res. 94, 925–956.

Guenther, A., Karl, T., Harley, P., Wiedinmyer, C., Palmer, P.I., Geron, C., 2006. Estimates of global terrestrial isoprene emissions using MEGAN model of emissions of gases and Aerosols from nature. Atmos. Chem. Phys. 6, 3181–3210. http://dx.doi.org/10.5194/acp-6-3181-2006.

Huang, C., Chen, C.H., Li, L., Cheng, Z., Wang, H.L., Huang, H.Y., Streets, D.G., Wang, Y.J., Zhang, G.F., Chen, Y.R., 2011. Emission inventory of anthropogenic air pollutants and VOCs species in the Yangtze River Delta region, China. Atmos. Chem. Phys. 11, 4105–4120.

Huang, J.P., Zhou, C.H., Lee, X.H., Bao, Y.X., Zhao, X.Y., Fung, J., Richter, A., Liu, X., Zheng, Y.Q., 2013. The effects of rapid urbanization on the levels in tropospheric nitrogen dioxide and ozone over East China. Atmos. Environ. 77, 558–567.

Kim, S., Byun, D.W., Cohan, D., 2009. Contributions of inter- and intra-state emissions to ozone over Dallas-Fort Worth, Texas. Civ. Eng. Environ. Syst. 26, 103–116.

Li, L., Chen, C.H., Huang, C., Fu, J., Streets, D.G., Huang, H.Y., Zhang, G.F., Wang, Y.J., Jang, C.J., Wang, H.L., Chen, Y.R., Fu, J.M., 2011a. Air quality and emissions in the Yangtze River Delta. Atmos. Chem. Phys. 11, 1621–1639.

Li, L., Chen, C.H., Huang, C., Huang, H.Y., Zhang, G.F., Wang, Y.J., Chen, M.H., Wang, H.L., Chen, Y.R., Streets, D.G., Fu, J.M., 2011b. Ozone sensitivity analysis with the MM5-CMAQ modeling system for Shanghai. J. Environ. Sci. 23, 1150–1158.

Li, L., Chen, C.H., Huang, C., Huang, H.Y., Zhang, G.F., Wang, Y.J., Wang, H.L., Lou, S.R., Qiao, L.P., Zhou, M., Chen, M.H., Chen, Y.R., Streets, D.G., Fu, J.S., Jang, C.J., 2012a. Process analysis of regional ozone formation over the Yangtze River Delta, China using the community multi-scale air quality modeling system. Atmos. Chem. Phys. 12, 10971–10987.

Li, Y., Lau, A.K.H., Fung, J.C.H., Zheng, J.Y., Zhong, L.J., Louis, P.K.K., 2012b. Ozone Source Apportionment (OSAT) to differentiate local regional and super-regional source contributions in the Pearl River Delta region, China. J. Geo. Res. 117, D15305. http://dx.doi.org/10.1029/2011JD017340.

Li, Y., Lau, K.H.A., Fung, C.H.J., Ma, H., Tse, Y.Y., 2013. Systematic evaluation of ozone control policies using an Ozone Source Apportionment method. Atmos. Environ. 76, 136e-146.

Liu, X.H., Zhang, Y., Cheng, S.Y., Xing, J., Zhang, Q., Streets, D.G., Jang, C., Wang, W.X., Hao, J.M., 2010. Understanding of regional air pollution over China using CMAQ, part I: performance evaluation and seasonal variation. Atmos. Environ. 44, 2415–2426.

Liu, T., Li, T.T., Zhang, Y.H., Xu, Y.J., Lao, X.Q., Rutherford, S., Chu, C., Luo, Y., 2013. The short-term effect of ambient ozone on mortality is modified by temperature in Guanzhou, China. Atmos. Environ. 76, 59–67.

Marais, E.A., Jacob, D.J., Wecht, K., 2014. Anthropogenic emissions in Nigeria and implications for atmospheric ozone pollution: a view from space. Atmos. Environ. 99, 32–40.

Michalakes, J., Chen, S., Dudhia, J., Hart, L., Klemp, J., Middlecoff, J., Skamarock, W., 2001. In: Zwieflhofer, Walter, Kreitz, Norbert (Eds.), Development of a Next Generation Regional Weather Research and Forecast Model. Developments in Teracomputing: Proceedings of the Ninth ECMWF Workshop on the Use of High Performance Computing in Meteorology. World Scientific, Singapore, pp. 269–276.

National Bureau of Statistics of China, China (Ed.) (NBSC) (2013), China Statistical yearbook 2013. China Statistics Press, Beijing (in Chinese).

Qiao, Y.Z., Wang, H.L., Huang, C., Chen, C.H., Su, L.Y., Zhou, M., Xu, H., Zhang, G.F., Chen, Y.R., Li, L., Chen, M.H., Huang, H.Y., 2012. Source profile and chemical reactivity of volatile organic compounds from vehicle exhaust. Huanjing Kexue 33, 1071–1079.

Shao, M., Tang, X.Y., Zhang, Y.H., Li, W.J., 2006. City clusters in China: air and surface water pollution. Front. Ecol. Environ. 4 (7), 353–361.

Shi, C.Z., Wang, S.S., Liu, R., 2015. A study of aerosol optical properties during ozone pollution episodes in 2013 over Shanghai, China. Atmos. Res. 153, 235–249.

Streets, D.G., Fu, J.S., Jang, C.J., Hao, J.M., He, K.B., Tang, X.Y., Zhang, Y.H., Wang, Z.F., Li, Z.P., 2007. Air quality during the 2008 beijing olympic games. Atmos. Environ. 41, 480–492.

Wang, X.S., Li, J.L., Zhang, Y.H., Xie, S.D., Tang, X.Y., 2009. Ozone source attribution during a severe photochemical smog episode in Beijing, China. Sci. China Ser. B Chem. 39, 548–559 (in Chinese).

Wang, L.T., Jang, C., Zhang, Y., Wang, K., Zhang, Q., Streets, D.G., Fu, J., Lei, Y., Schreifels, J., He, K.B., Hao, J.M., Lam, Y.F., Lin, J., Meskhidze, N., Voorhees, S., Evarts, D., Phillips, S., 2010. Assessment of air quality benefits from national air pollution control policies in China. Part II: evaluation of air quality predictions and air quality benefits assessment. Atmos. Environ. 44, 3449–3457.

Wang, H.L., Qiao, Y.Z., Chen, C.H., Lu, J., Dai, H.X., Qiao, L.P., Lou, S.R., Huang, C., Li, L., Jing, S.A., Wu, J.P., 2014a. Source profiles and chemical reactivity of volatile organic compounds from solvent use in Shanghai, China. Aerosol Air Qual. Res. 14, 301–310.

Wang, H.L., Lou, S.R., Huang, C., Qiao, L.P., Tang, X.B., Chen, C.H., Zeng, L.M., Wang, Q., Zhou, M., Lu, S.H., Yu, X.N., 2014b. Source profiles of volatile organic compounds from biomass burning in Yangtze River Delta, China. Aerosol Air Qual. Res. 14 (3), 818–828.

Wikipedia. Available at: http://zh.wikipedia.org/wiki/%E4%B8%AD%E5%9B%BD%E7%9C%81%E7%BA%A7%E8%A1%8C%E6%94%BF%E5%8C%BA%E9%9D%A2%E7%A7%AF%E5%88%97%E8%A1%A8(2014/10/29).

Xie, M., Zhu, K.G., Wang, T.J., Yang, H.M., Zhuang, B.L., Li, S., Li, M.G., Zhu, X.S., Ouyang, Y., 2014. Application of photochemical indicators to evaluate ozone nonlinear chemistry and pollution control countermeasure in China. Atmos. Environ. 99, 466–473.

Xing, J., Wang, S.X., Jang, C., Zhu, Y., Hao, J.M., 2011. Nonlinear response of ozone to precursor emission changes in China: a modeling study using response surface methodology. Atmos. Chem. Phys. 11, 5027–5044.

Yarwood, G., Morris, R., Yocke, M., Hogo, H., Chico, T., 1996. Development of a methodology for source apportionment of ozone concentration estimates from a photochemical grid model. In: Presented at the 89th Annual Meeting. Air & Waste Management Association, Nashville Tenn.

Yarwood, G., Roa, S., Yocke, M., and Whitten, G. (2005), Updates to the Carbon Bond Chemical Mechanism: CB05. Final report to the US EPA, RT-0400675, available at: http://www.camx.com.

Zhang, Y., Vijayaraghavan, K., Seigneur, C., 2005. Evaluation of three probing techniques in a three-dimensional air quality model. J. Geophys. Res. Atmos, 110, D02305.

Zhang, Q., Streets, D.G., Carmichael, G.R., He, K.B., Huo, H., Kannari, A., Klimont, Z., Park, I.S., Reddy, S., Fu, J.S., Chen, D., Duan, L., Lei, Y., Wang, L.T., Yao, Z.L., 2009. Asian emissions in 2006 for the NASA INTEX-B mission. Atmos. Chem. Phys. 9, 5131–5153.

Zhang, Y.N., Xiang, Y.R., Chan, L.Y., Chan, C.Y., Sang, X.F., Wang, R., Fu, H.X., 2011. Procuring the regional urbanization and industrialization effect on ozone pollution in Pearl River Delta of Guangdong, China. Atmos. Environ. 28 (45), 4898–4906.